COMPARISON OF RUC CONDENSATE ANALYSES AND FORECASTS WITH SATELLITE-DERIVED CLOUD PROPERTIES

William L. Smith Jr., Patrick Minnis
Science Directorate, NASA Langley Research Center, Hampton, VA

Stanley G. Benjamin
NOAA Earth System Research Laboratory, Boulder, CO

1. INTRODUCTION

The transportation industry, including aviation, has an important need for improved predictions of clouds, fog, ceiling/visibility and precipitation. Because clouds play a crucial role in the dynamics and thermodynamics of the atmosphere, they must be accounted for in numerical prediction models that weather forecasters rely on for guidance. Despite significant advances in our understanding of clouds, particularly their microphysical and radiative processes, many problems remain in adequately representing cloud microphysics in models, either explicitly or implicitly thru parameterizations (Khain et al., 2000). The operational NOAA Rapid Update Cycle (RUC) model employs an hourly assimilation cycle to provide regional weather analyses and forecasts (Benjamin et al., 2004a). The RUC cycles at full-resolution five microphysical species (cloud water, cloud ice, rain water, snow, and graupel) and has the capability for updating these fields from observations. The RUC is a key component of the FAA Aviation Weather Research Progam (AWRP) focused on improved aviation safety and flight planning over the continental USA (CONUS). The RUC model output provide critical elements to AWRP products that include aircraft icing conditions, flight altitude winds and temperatures, and precipitation, to name a few. Accurate model predictions of these elements require accurate specification of cloud and hydrometeor fields in the model initial conditions.

Satellite remote sensing can provide observations of cloud properties. Solar reflectance techniques based on the pioneering work by Nakajima and King (1990) make it possible to derive cloud microphysical properties (e.g. particle size, number concentration, water

path) from satellite data along with macrophysical properties such as cloud cover and height. Currently, hourly 4-8 km resolution cloud properties are being generated at NASA Langley research Center (LaRC) under the NASA Advanced Satellite Aviation-weather Products (ASAP) Initiative (Minnis et al., 2004a). The parameters include liquid and ice water path (IWP and LWP), cloud top height, cloud droplet effective radius r_{eff}, and icing probability and intensity among other parameters. These products are being integrated into the AWRP Current Icing Potential (CIP) product to complement the RUC output and pilot Reports (PIREPS) currently being used to produce the CIP. The LaRC products are based on near-real time analyses of Geostationary Operational Environmental Satellite (GOES) radiances and represent a significant advance in quantifying cloudiness in near-real time at high temporal and spatial resolutions. Recent comparisons of the satellite-derived cloud parameters with aircraft measurements and retrievals from ground-based passive and active sensors are favorable (Dong et al., 2002, Min et al., 2004, Mace et al., 2005). This suggests that satellite derived cloud parameters have the potential to improve NWP analyses and forecasts either indirectly, via intercomparisons that identify model deficiencies, or directly, via satellite data assimilation. The RUC currently assimilates a variety of data to analyze cloud parameters. These include a cloud top pressure and temperature product based on satellite data, surface METAR cloud, ceilometer and visibility observations and radar reflectivity. In addition, plans are being developed to assimilate the LaRC products since LWP and IWP interpreted with state-of-the-art models can provide cloud thickness and hydrometeor constraints that are unavailable from the NESDIS cloud-top product, the GOES radiances, or from the surface observations.

In this paper, the RUC model output is evaluated in terms of the analyzed and predicted

---

Corresponding author address: William L. Smith Jr., NASA Langley Research Center, Hampton, VA., 23681.   (email:w.l.smith@larc.nasa.gov)

condensate fields by comparing them directly to the LaRC satellite-derived cloud products and quantifying the differences. Such a comparison will help guide the assimilation effort and provide a benchmark for future model evaluations.

2. DATA AND METHODOLOGY

The datasets analyzed in this study comprised 36 days of coincident RUC output and LaRC satellite products for the period between between May 10 and July 13, 2005 .

The satellite products were derived operationally over the CONUS utilizing half-hourly, 4km resolution GOES-10 and GOES-12 data. The GOES-10 at 135°W measures radiances at 0.65, 3.9, 10.8, and 12 μm. GOES-12 at 75°W has similar channels with the exception of a 13.3-μm channel in place of the 12 -μm channel. GOES-12 data are analyzed over an area between 65°W and 105°W, while the GOES-10 data cover 90°W to 125°W. The results are stitched together at 99°W. Surface type, clear-sky albedo, and surface emissivity maps are used to estimate the cloud-free radiances for a given scene as described by Minnis et al. (2001, 2004b). A set of decision trees, based on all four channels, is then employed to identify the cloudy pixels. During the daytime, cloud properties are determined by matching GOES radiance observations for cloudy pixels at 0.63, 3.9, 10.8 and 12.0 μm to parameterizations of model calculations of cloud emittance and reflectance for a wide range of water droplet and ice particle sizes (Minnis et al, 1998). The method provides estimates of the effective cloud temperature T_c, cloud height z and thickness h, phase, optical depth OD, effective droplet radius or effective ice crystal diameter. LWP or IWP are estimated from the OD and effective particle size depending on the retrieved phase at cloud top. A similar technique is employed at night, however the cloud microphysical properties are less certain overall since only infrared channels are available and the radiances are relatively insensitive to cloud microphysics when the clouds are optically thick. Currently, the operational CONUS products are derived for every other pixel due to limited computational resources. This yields an effective 8 km resolution for the satellite products. More detail on the cloud property retrieval algorithm can be found in Minnis et al., 2004b and references therein.

The RUC data were obtained via ftp from the National Center for Environmental Prediction (NCEP). On June 28, 2005 at 1200 UTC, the 13 km version of RUC (RUC13) became operational and is included in the comparisons shown below. Prior to June 28, we used the available 20 km version (RUC 20). The RUC output includes analyzed and predicted fields of five microphysical species (cloud water, cloud ice, rain water, snow, and graupel) at up to 50 vertical levels. Cloud top phase is determined by the species analyzed or predicted at the highest cloud level. Cloud top height is also determined from the model output. The total water path from the RUC is computed by vertically integrating the total densities for all five species. This allows for direct comparison with the satellite-derived water path which is an integrated quantity representing the total column cloud water.

In the analysis presented here, cloud properties analyzed and predicted by RUC are compared with the satellite estimates. The comparison is focused on cloud frequency, cloud water path and cloud top height. The analysis is restricted to satellite products derived at 1445, 1745 and 2045 UTC, and analyzed and predicted (1, 3, and 6 hour forecast) fields from the RUC valid at 1500, 1800 and 2100 UTC. Spatial matching is accomplished by mapping the satellite pixel level parameters to the RUC grid. For each grid box, the satellite pixel-level parameters are averaged for the ice and liquid phases separately. A RUC grid box is either cloudy or clear. A corresponding GOES grid box is either overcast, clear or partly cloudy. Cloud frequencies are computed for overcast grid boxes, and broken down into levels; low (0-3 km), mid (3-7 km) and high (greater than 7 km), as well as stratified by the phase at cloud top.

3. RESULTS

Examples of the GOES and RUC cloud analyses are shown in figures 1 and 2 for June 29, 2005. The GOES analysis was performed on the 1745 UTC GOES-10 and GOES-12 data while the RUC data are from the 1800 UTC analysis. Figure 1a and 1b depict the GOES 10.8 μm temperature and 0.63 μm reflectance, respectively. Low clouds identified by their warm temperatures and bright reflectances cover much of the eastern pacific and are also found over southeastern Ontario. Low cumulus

clouds blanket much of the Ohio and Missouri valleys stretching southwestward into eastern Texas. High clouds associated with a low pressure system over South Dakota cover much of northern Plains and south-central Canada. High clouds are also found over much of the eastern seaboard stretching through the gulf of Mexico into northeast Mexico. The southwestern U.S. is primarily free of cloud. The cloud phase retrieved from GOES is shown in figure 1c and depicts clear areas in green, warm liquid clouds in blue, super-cooled liquid clouds in cyan and high clouds in red. Close inspection of the imagery reveal that the LaRC cloud analysis appears to perform exceptionally well in identifying clouds. The RUC cloud analysis is shown in Figure 1d with a similar color scale. High clouds associated with the storm over the northern plains and found over the eastern seaboard are well captured, although there appear to be too many high clouds analyzed by the RUC over the Ohio valley and western Gulf of Mexico. Large areas of stratocumulus over the eastern Pacific are not captured by the RUC-13. This problem appears to be specific to RUC-13 and was not evident in the RUC-20 cases examined prior to the RUC-13 implementation on June 28. Some of the low clouds over southern Ontario and much of the cumulus in the Ohio and Missouri valleys are not well captured in the RUC analysis. Cloud water path determined from GOES and RUC are shown in Figure 2a and 2b, respectively. Except for the problem over the eastern pacific, the comparison looks reasonable over much of the domain. However, a difference image (GOES minus RUC) shown in figure 2c reveals large regional water path differences on the order of several thousand g/m^2. For example, there appears to be significant convection over the northern gulf, just south of New Orleans. The RUC depicts water paths in this region on the order of 300 g/m^2 whereas the GOES indicate values greater than 2000 g/m^2. Some of this difference could be attributed to navigation and/or parallax error in the satellite geo-rectification that could be on the order of 10km and should be accounted for in future comparisons. However, the scale of the difference patterns in figure 2c appear to be at least an order of magnitude larger than this in most cases.

Figure 3 depicts the frequency of occurrence, in percent, of overcast grid cells for four cloud scenarios; (1) all overcast cloud regions, (2) overcast ice cloud regions, (3) overcast liquid cloud regions, and (4) overcast regions consisting of ice and liquid. Values are computed for GOES and for the RUC analyses, 1, 3 and 6-hour forecasts for all the data in the 36 day period analyzed here. Figure 3a (3b) show the comparison for RUC-20 (RUC-13) determined from the days analyzed before (after) the RUC-13 implementation. For all clouds and liquid clouds, the RUC-20 analyses and forecasts agrees with GOES within a few percent. Ice cloud frequency in the RUC analysis (forecasts) exceeds GOES by about 5 (10 %). The comparison with RUC-13 is not as good. There are 6% fewer overcast liquid cloud regions in RUC-13 than determined from GOES and nearly 20% more ice cloud. For all clouds, the RUC-20 exceeds the GOES results by 4-8 %.

In order to gain some knowledge of regional cloudiness differences, the frequency of occurrence of RUC overcast and clear regions is computed for regions the GOES analyses indicate to be 100% overcast. The results are shown in Figure 4. The results indicate that for overcast GOES regions, the RUC-20 (RUC-13) analysis is also overcast 77% (76%) of the time. The other 23% (24%) of the time, the RUC regions are clear. Similar values are found in the RUC-13 forecasts, which offer about a 4-9 % improvement over the RUC-20. Figure 5 is similar to figure 4, but here the frequency histograms are computed for 100% clear regions as determined from GOES. The RUC-20 analyses are found to be clear when GOES is clear about 93 % of the time. In contrast, the RUC-13 is found to be clear only 80% of the time that GOES indicates clear.

A comparison of the cloud top phase determined by the RUC and from the LaRC GOES algorithm is depicted in figures 6 and 7. Figure 6 depicts the frequency of overcast ice, liquid, mixed, and clear regions determined by the RUC for all GOES regions determined to be overcast with ice clouds. Here, the RUC-13 indicates much better agreement with GOES than the RUC-20. In the RUC-20 analyses, ice cloud is found only 69% of the time that GOES indicates overcast ice. In comparison, the RUC-13 value is 89%. Relative to GOES-derived ice clouds, RUC-13 has more ice couds and less liquid cloud and clear areas than the RUC-20. It should be noted that the RUC-13 forecasts do degrade with increasing lead time. For example, the RUC-13 6-hour forecast only indicates 66% ice cloud cover and 22% clear when GOES is ice cloud overcast. Figure 7 is similar to figure

6, but here the frequency histograms are computed for 100% liquid cloud overcast as determined from GOES. In this case, only 54% (36%) of the regions are found to be overcast and 29%) (42%) of the regions are found to be clear in the RUC-20 (RUC-13).

A similar analysis to that shown in figures 6 and 7 was conducted by stratifying the clouds into three levels (low, mid and high), rather than stratifying by phase. The results (not shown here) were similar to the phase results owing to the fact that most low clouds are water clouds and most high clouds are ice clouds.

Figure 8a and 8b depict frequency histograms of ice and liquid water path differences (RUC minus GOES), respectively. The distributions are roughly Gaussian with the exception of significant peaks at the ends of the ice water path plot. The peak in both difference plots is found to be below zero. The water path means, bias and rms differences are shown in tables 1 and 2. For the RUC-20 analyses, the IWP (LWP) is on average 259 g/m^2 (57 g/m^2) lower than the GOES-derived values. In both cases, the biases represent about 50% of the mean GOES values. Note that the ice cloud water path bias is substantially reduced in the RUC-13.

Figure 9a and 9b depict frequency histograms of ice and liquid cloud top height differences (RUC minus GOES), respectively. The distributions are roughly Gaussian. The peak in the ice (liquid) cloud top height is found to be less (greater) than zero. The cloud height means, bias and rms differences are shown in tables 1 and 2. For the RUC-20 analyses, the ice (liquid) cloud top height is on average 0.5 km higher (lower) than the GOES-derived values. In both cases, the biases represent about 50% of the mean GOES values. In RUC-13, the ice cloud top height bias nearly doubles while the liquid cloud top height bias is cut in half.

4.   CONCLUDING REMARKS

The results presented here utilize new satellite derived cloud parameters to provide a preliminary assessment of the condensate fields analyzed and forecasted by the RUC-20 and RUC-13. In many cases, these comparisons reveal large differences in modeled cloud parameters versus those derived from satellite observations that significantly exceed the uncertainties in the satellite analyses, implying that the assimilation of observed cloud properties is needed. This is not unexpected given the known complexity of cloud microphysical processes, yet crude representation in all numerical weather prediction models. Some of the key findings of this study are: The frequency of overcast cloud analyzed and predicted by the RUC-20 agrees well with the GOES results. RUC-13 appears to overestimate ice cloud cover. RUC-13 also produces more clouds than RUC-20 when GOES indicates clear. However, when considering only overcast cloud regions as determined from GOES, the RUC only produces overcast clouds about 75% of the time. This implies that although the total RUC cloud cover may be reasonable or even greater than GOES overall, clouds are often in the wrong location. This scenario appears worse for RUC-13 than RUC-20. For GOES overcast ice cloud regions, the RUC-13 produces more ice cloud than the RUC-20. For GOES overcast liquid cloud regions, the RUC-13 (RUC-20) analyses only produce liquid clouds 36 % (54%) of the time and produce clear regions 42 % (29%) of the time. The decreased skill in the RUC-13 appears to be related to the lack of oceanic stratus in the RUC-13 analyses. On average GOES derived ice and liquid water paths are about twice as large as those produced by RUC. The LaRC satellite products should prove useful in further understanding these differences. The results presented here should also help guide future assimilation efforts and provide a benchmark for future model evaluations.

References

Benjamin, S. G., D. Dévényi, S. S. Weygandt, K. J. Brundage, J. M. Brown, G. A. Grell, D. Kim, B. E. Schwartz, T. G. Smirnova, and T. L. Smith, and G. S. Manikin, 2004a: An hourly assimilation-forecast cycle the RUC. *Mon. Wea. Rev.*, **132**, 495-518.

Dong, X., P. Minnis, G. G. Mace, W. L. Smith Jr., M. Poellot, R. Marchand, and A. Rapp, 2002: Comparison of stratus cloud properties deduced from surface, GOES, and aircraft data during the March 2000 ARM Cloud IOP. *J. Atmos. Sci.,* **59,** 3265–3284.

Khain, A., M. Otchinnikov, M. Pinsky, A. Pokrovsky, H. Krugliak, 2000: Notes on the state-of-the-art numerical modeling of cloud microphysics. *Atmos. Res.*, **55**, 159-224.

Mace, G. G., Y. Zhang, S. Platnick, M. D. King, P. Minnis, and P. Yang, 2005: Evaluation of cirrus cloud properties from MODIS radiances using cloud properties derived from ground-based data collected at the ARM SGP site. J. Appl. Meteorol., **44**,221-240.

Min, Q, P. Minnis, and M. M. Khaiyer, 2004: Comparison of cirrus optical depths from GOES-8 and surface measurements. J. Geophys. Res., **109**, No. D15, D15207 10.1029/2003JD004390, August 12.

Minnis, P., et al., 2001: A near-real time method for deriving cloud and radiation properties from satellites for weather and climate studies. Proc. AMS 11th Conf. Satellite Meteorology and Oceanography, Madison, WI, Oct. 15-18, 477-480.

Minnis, P., L. Nguyen, W. L. Smith, Jr., M. M. Khaiyer, R. Palikonda, D. A. Spangenberg, D. R. Doelling, D. Phan, G. D. Nowicki, P. W. Heck, and C. Wolff, 2004a: Real-time cloud, radiation, and aircraft icing parameters from GOES over the USA. Proc. 13th AMS Conf. Satellite Oceanogr. and Meteorol., Norfolk, VA, Sept. 20-24, CD-ROM, P7.1.

Minnis, P., D. F. Young, S. Sun-Mack, Q. Z. Trepte, R. R. Brown, S. Gibson, and P. Heck, 2004b: Diurnal, seasonal, and interannual variations of cloud properties derived for CERES from imager data. Proc. 13th AMS Conf. Satellite Oceanogr. and Meteorol., Norfolk, VA, Sept. 20-24, CD-ROM, P6.10.

Nakajima, T., and M. D. King, 1990: Determination of the optical thickness and effective particle radius of clouds from reflected solar radiation measurements. Part I: Theory. *J. Atmos. Sci., 47,* 1878-1893.
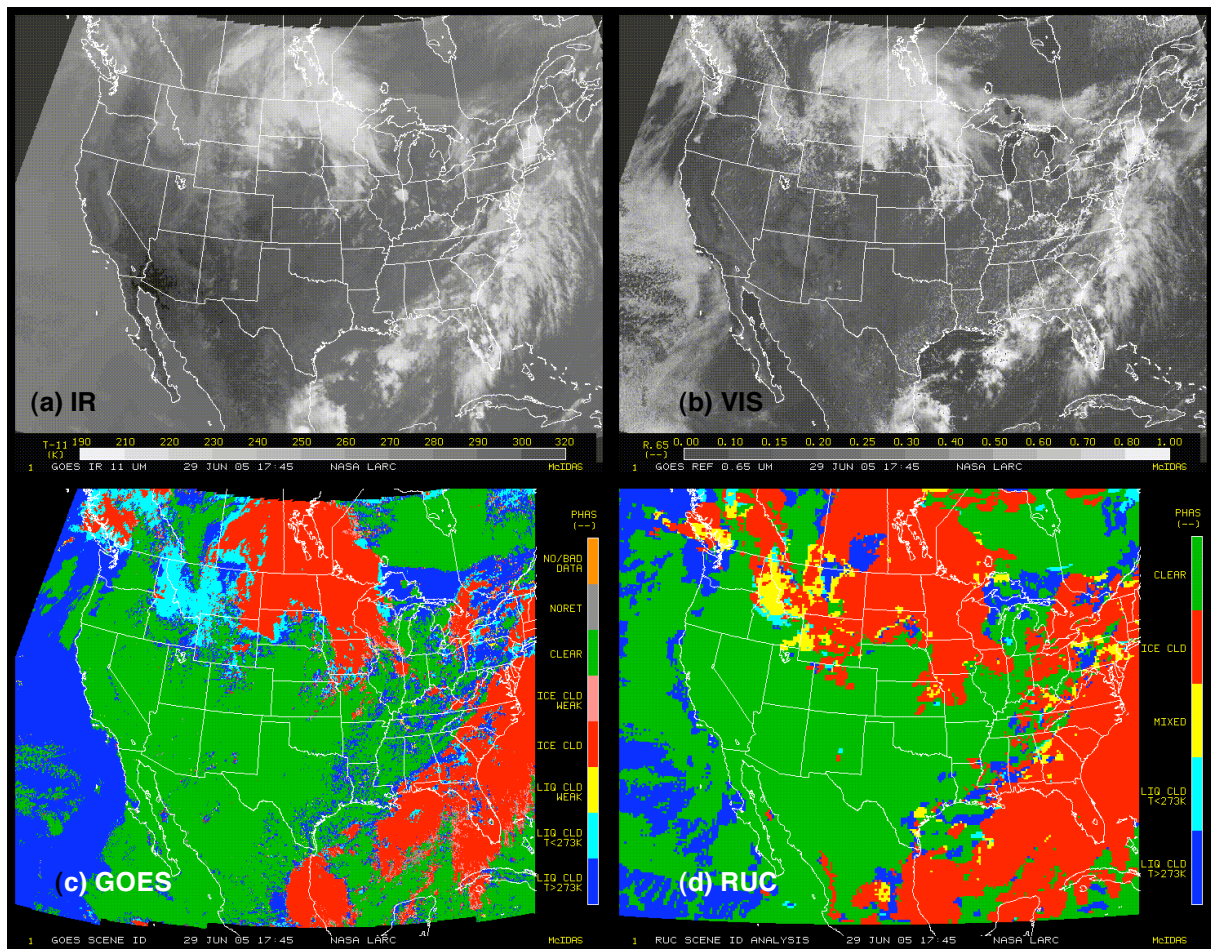
Fig 1. GOES 10.8 μm image (a), 0.63 μm image (b), Cloud top phase derived from GOES (c) and determined by the RUC (d) on June 29, 2005 at 1745 UTC.
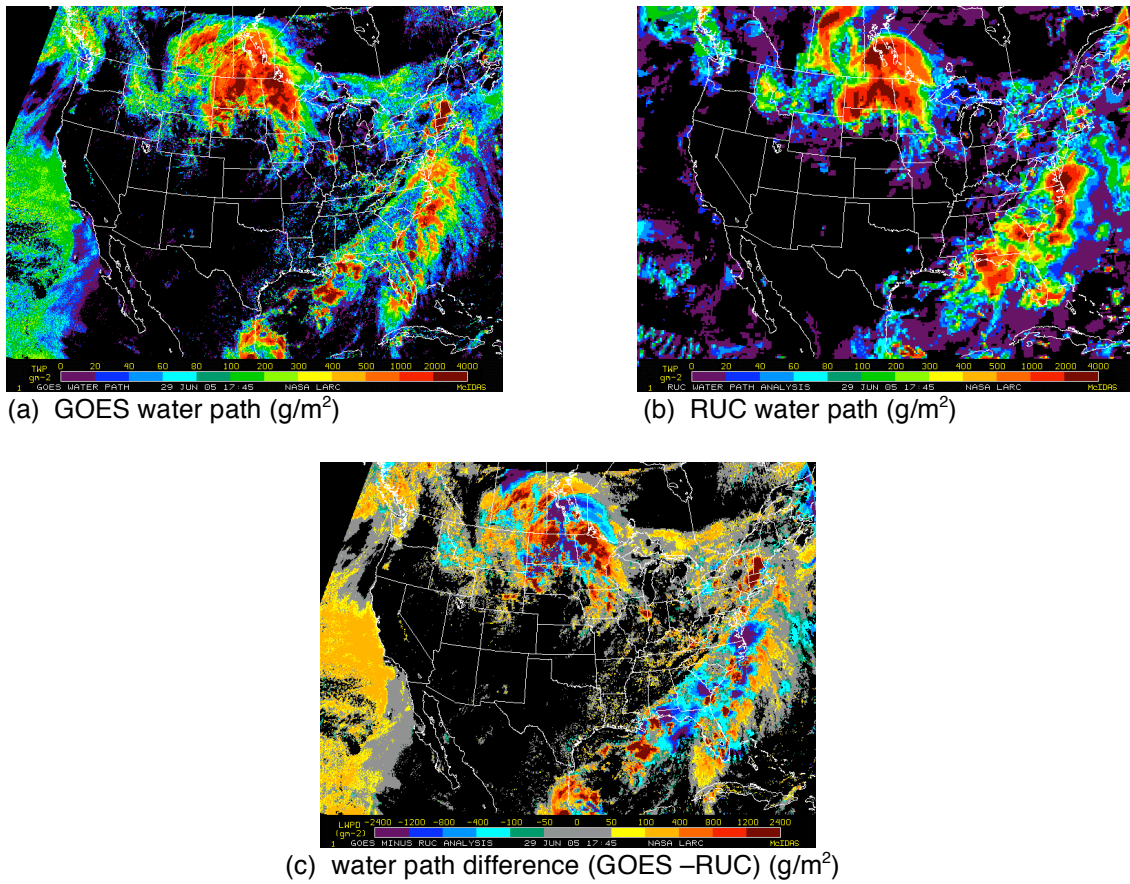
(a) GOES water path (g/m^2)

(b) RUC water path (g/m^2)

(c) water path difference (GOES –RUC) (g/m^2)

Fig 2. GOES (a) and RUC (b) water path and water path difference (c) for June 29, 2005 at 1745
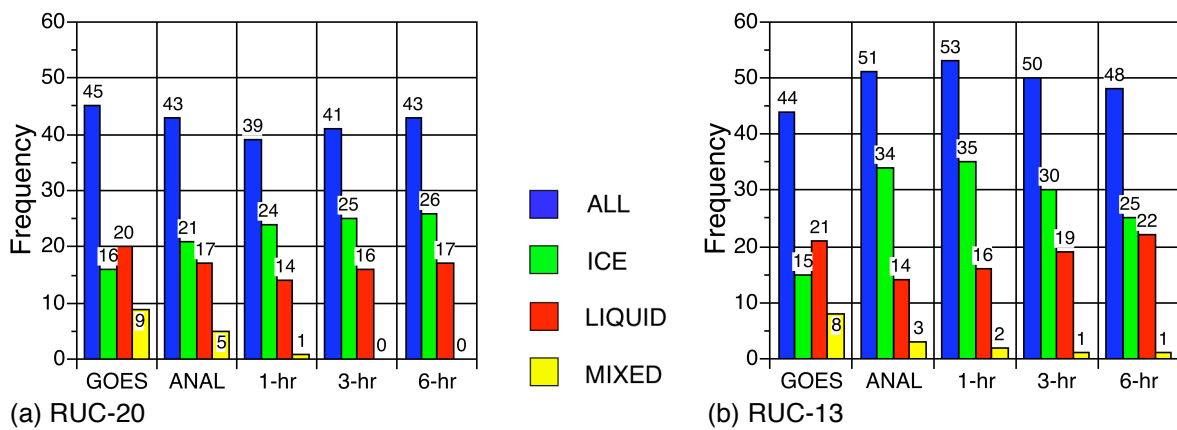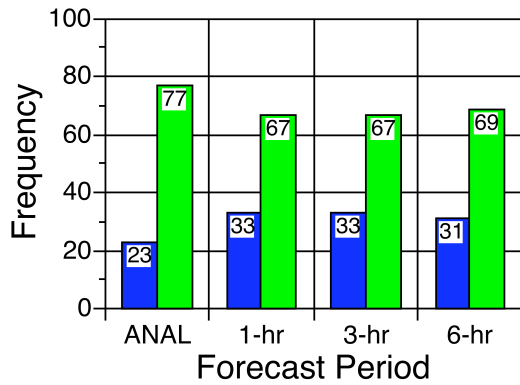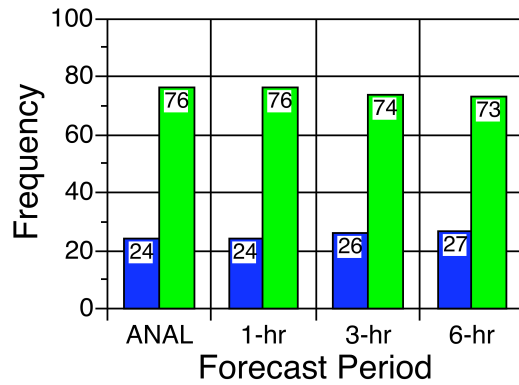

(a) RUC-20

(b) RUC-13

Fig 3. Frequency of occurrence (%) of overcast grid cells for all clouds, ice clouds, liquid clouds and regions with ice and liquid (mixed) for the period before (a) and after (b) the RUC 13 implementation. The first grouping represents the GOES results followed by the RUC analyses and forecasts.

(a) RUC-20 (b) RUC-13

RUC CLEAR %   RUC CLOUD %

Fig 4. Frequency (%) histograms of RUC clear and cloudy regions for regions determined to be 100% cloudy in the GOES analysis.
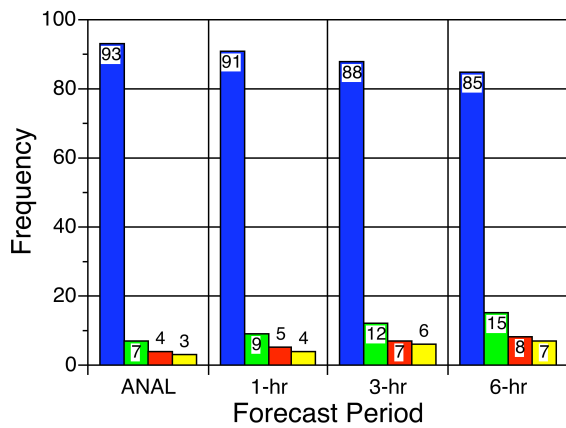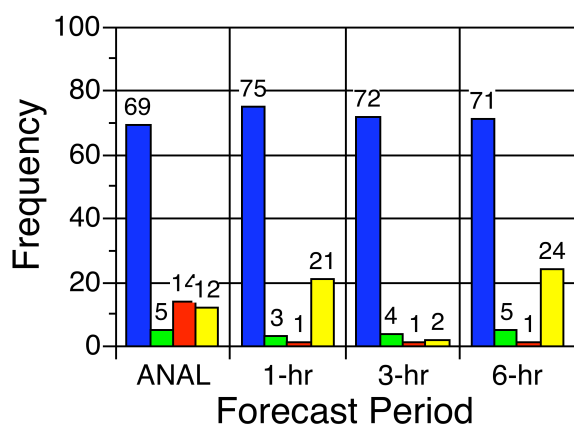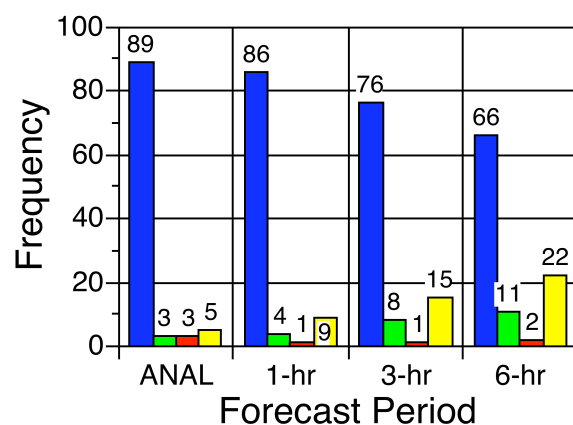

(a) RUC-20 (b) RUC-13
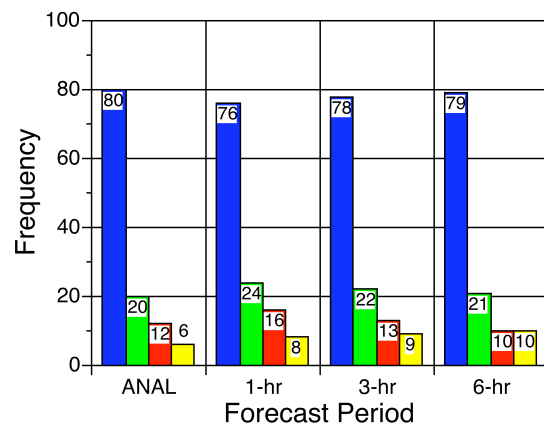
RUC CLEAR %   RUC CLOUD %

Fig 5. Frequency (%) histograms of RUC clear and cloudy regions for regions determined to be 100% clear in the GOES analysis. The overcast ice and liquid cloud frequencies are depicted in red and yellow, respectively.
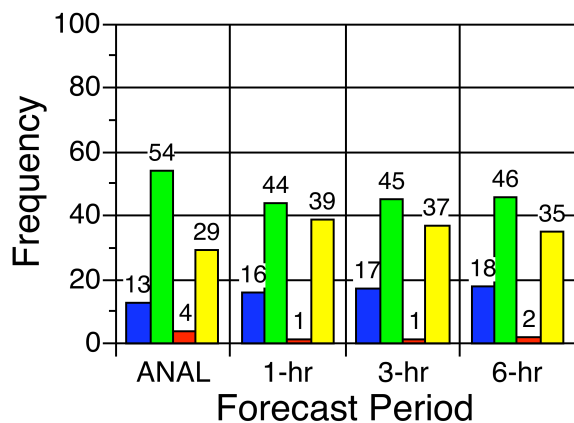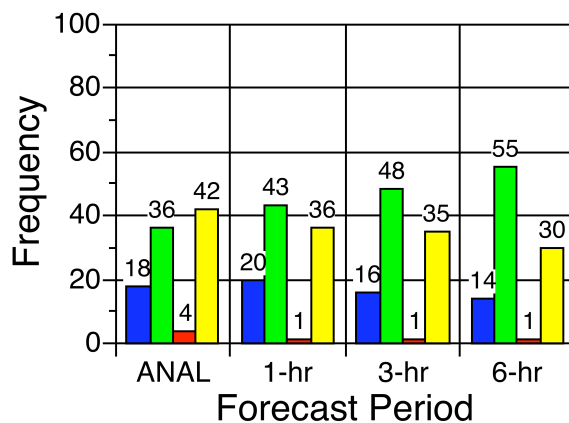
Fig 6. Frequency (%) histograms of RUC clear and cloudy conditions for regions determined to be 100% overcast ice cloud in the GOES analysis.

Fig 7. Frequency (%) histograms of RUC clear and cloudy conditions for regions determined to be 100% overcast liquid water cloud in the GOES analysis.
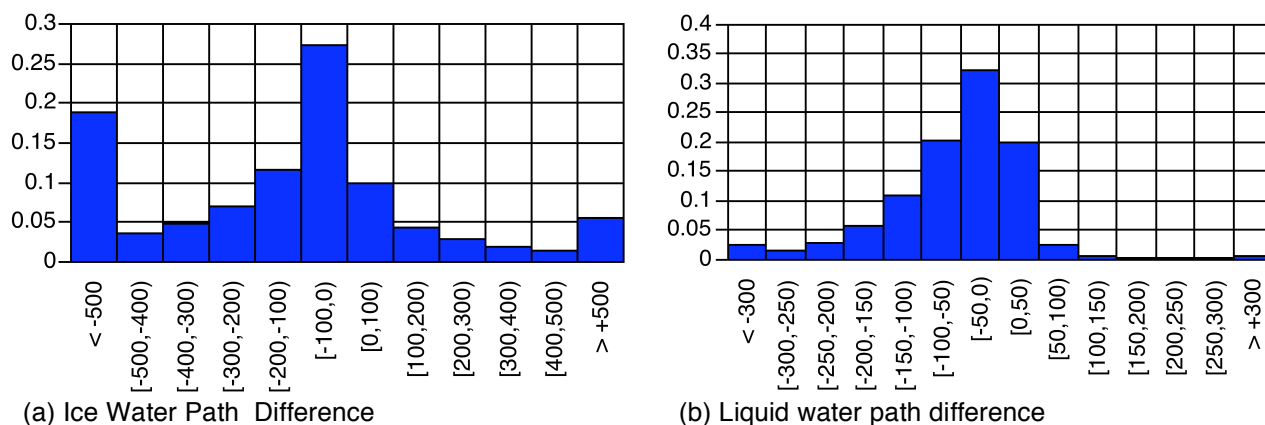
(a) Ice Water Path Difference

(b) Liquid water path difference

Fig 8. Frequency histograms of (a) ice water path and (b) liquid water path differences (RUC minus GOESanalysis) in g/m^2.

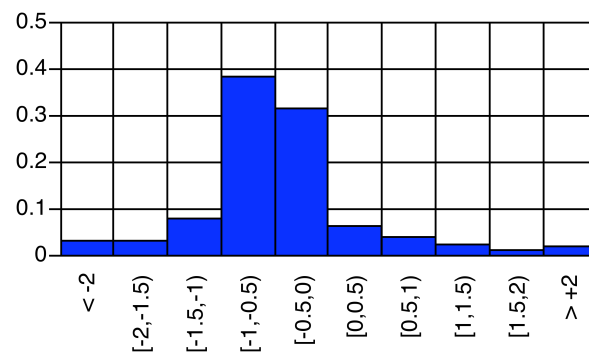Table 1. RUC-20 ice water path comparison with GOES. RUC-13 shown in parentheses (g/m^2).

	RUC	GOES	BIAS	RMSD
ANALYSIS	259 (321)	518 (499)	-259 (-178)	706(829)
1-hour Fcst	253 (348)	486 (506)	-233 (-156)	669 (845)
3-hour Fcst	301 (342)	496 (526)	-196 (-184)	685 (863)
6-hour Fcst	292 (353)	480 (537)	-188 (-184)	672 (873)

Table 2. RUC-20 liquid water path comparison with GOES. RUC-13 shown in parentheses (g/m^2).

	RUC	GOES	BIAS	RMSD
ANALYSIS	57 (57)	114 (116)	-57 (-59)	123 (134)
1-hour Fcst	47 (46)	115 (119)	-69 (-72)	132 (139)
3-hour Fcst	58 (68)	120 (121)	-62 (-53)	133 (144)
6-hour Fcst	65 (76)	118 (119)	-53 (-43)	129 (132)
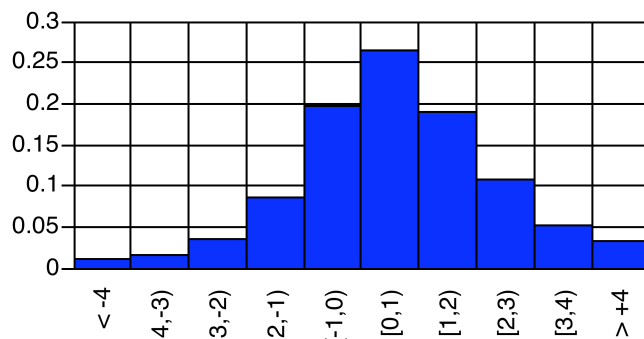
(a) Ice cloud top height difference

(b) Liquid cloud top height difference

Fig 9. Frequency histograms of (a) ice cloud top height and (b) water cloud top height differences (GOES minus RUC analysis) in km.

Table 3. RUC-20 ice cloud top height comparison with GOES. RUC-13 shown in parentheses (km).

	RUC	GOES	BIAS	RMSD
ANALYSIS	9.7 (10.5)	9.2 (9.7)	0.5 (0.9)	1.8 (2.0)
1-hour Fcst	9.7 (10.8)	9.0 (9.6)	0.6 (1.2)	2.1 (2.2)
3-hour Fcst	9.9 (10.7)	9.0 (9.5)	0.9 (1.1)	2.2 (2.2)
6-hour Fcst	10.1 (10.5)	8.9 (9.4)	1.2 (1.1)	2.3 (2.2)

Table 4. RUC-20 liquid cloud top height comparison with GOES. RUC-13 shown in parentheses (km).

	RUC	GOES	BIAS	RMSD
ANALYSIS	1.3 (1.4)	1.7 (1.6)	-0.5 (-0.2)	0.9 (1.1)
1-hour Fcst	1.0 (0.9)	1.7 (1.4)	-0.7 (-0.5)	1.0 (1.1)
3-hour Fcst	1.0 (0.8)	1.8 (1.4)	-0.7 (-0.6)	1.1 (1.0)
6-hour Fcst	1.0 (0.8)	1.7 (1.4)	-0.7 (-0.6)	1.0 (1.0)